

## Theory of Chemically Induced Dynamic Spin Polarization. 5. Orientation-Dependent Effects

Gary P. Zientara and Jack H. Freed\*

Department of Chemistry, Baker Laboratory, Cornell University, Ithaca, New York 14853 (Received July 11, 1979)

The Pedersen-Freed theory for chemically induced dynamic spin polarization CIDN(E)P is generalized to include the effects of anisotropic reactivities and anisotropic exchange interactions on the radical-pair mechanism. Detailed results are given for the simple case in which only one radical exhibits anisotropy that is approximated by a cosine distribution, and the rotational and translational motions are described by Brownian diffusion models. The primary effect upon CIDNP is the reduction in  $\Lambda$ , the reaction probability for the full collision. This effect can be rather accurately approximated by the use of an "effective" spherically symmetric specific rate constant, which depends, to some extent, on the rotational diffusion coefficient due to the effect of rotational relaxation. Thus CIDNP effects are rather well approximated by a spherically symmetric theory with a renormalized  $\Lambda$ . In the absence of reactivity, CIDEP effects for our model are reasonably well approximated by a spherically symmetric theory with a renormalized exchange interaction, especially for the asymptotic polarizations for large exchange interactions. When, however, there are orientation-dependent reactivities present with substantially greater orientation dependence than the exchange interaction, then significant deviations from a spherically symmetric theory are predicted even for asymptotic polarizations. The relationship to recent experiments is briefly discussed in this light. Anisotropic initial conditions are typically found to be relaxed by the effective rotational diffusion before they can substantially affect the CIDN(E)P observables.

### I. Introduction

The existing theories of chemically induced dynamic spin polarization were all developed for spherically symmetric interactions between the radical pairs.<sup>1,2</sup> Nevertheless, most interacting radicals are expected to display anisotropic features both in their ability to react and in their exchange features. In particular, the rate of reaction between nonspherical or bulky radicals is expected to be reduced by steric hindrance and other structural characteristics, including those of the solvent. Such effects have been confirmed experimentally in a recent CIDNP study,<sup>3</sup> and are otherwise well-known in many kinetic studies.

The matter of orientation-dependent effects upon radical (or molecule) reactivities has led to several theoretical studies. The general problem was first discussed by Solc and Stockmayer<sup>4</sup> in terms of a combined translational and orientation-dependent diffusion equation with reactive boundary conditions. They showed how the problem could be solved numerically in terms of Bessel function expansions (in radial space) and spherical Harmonic expansions (in orientation space). Freed and Pedersen<sup>2a</sup> suggested an approach closely related to that of Solc and Stockmayer but differing mainly in that finite differences are used in radial space to more easily deal with the short-range interactions that are so important in the CIDN(E)P phenomenon. Some later models were developed by others<sup>5,6</sup> to treat simplified cases, but the more realistic the model the greater is the reliance on numerical treatments<sup>4b,5</sup> or else considerable simplification of the model is required<sup>4a,6</sup> (e.g., simple two-state kinetic models for the orientation-dependent reactivity) and/or appeal to reencounter probabilistic arguments<sup>6</sup> rather than direct solution of the diffusion equation.

In this work, following the suggestions of Freed and Pedersen, we include the spin-dependent nature of the interacting radicals, i.e., their spin-dependent reactivity and exchange interactions, together with the diffusive aspects through the stochastic-Liouville formalism (SLE) in a combined approach by utilizing finite-differences (in radial space) and eigenfunction expansions (in orientation space). Thus, we are able to extend the theory of Pedersen

and Freed<sup>2</sup> for CIDN(E)P to cover orientation-dependent effects. Such calculations, dependent on several degrees of freedom (viz. spin, translational, and orientational), were virtually intractable by the earlier computational procedures, but they have now been easily performed by the use of newer methods developed by Zientara and Freed.<sup>7</sup>

The approach we use is a quite general one. It allows for orientation-dependent (1) initial conditions of the radical pair, (2) reactivities, and (3) spin-exchange interactions, while the radicals undergo both rotational and translational diffusion. Furthermore, while we do not explicitly consider such effects in this work, our approach can readily be extended to include orientation-dependent pair-potential effects (e.g. Coulombic and exchange interactions)<sup>2</sup> and hydrodynamic effects (e.g., Oseen's tensor<sup>2</sup>), as well as to orientation-dependent spin-relaxation effects (e.g., electron-spin dipolar interactions between the two radicals<sup>7</sup>). Nor do we include any orientation dependence in the size and shape of the radicals, features that are probably better dealt with by the methods of finite elements.<sup>7b</sup>

Our explicit calculations in the present work have been performed for rather simple forms for the angular dependence of reactive and exchange effects to maintain convenience in computation and simplicity in analysis. In particular, we compare our orientation-dependent results with the past studies based upon spherically symmetric interactions. Our results are generally consistent with the qualitative predictions of Pedersen and Freed.<sup>2</sup> That is, we find that CIDNP is mainly affected through the reduction in product yield due to the reduced range of orientations over which reaction can occur. The CIDEP results depend significantly upon the orientation dependence of the exchange interaction, but the range of magnitudes of the predicted polarizations is similar to what was found in the earlier studies with symmetric interactions.<sup>2</sup> The interpretation of these results, however, must now include the concept of a rotational-reencounter mechanism. This mechanism will be most effective in the limit where rotational diffusion is the dominant process of modulating the exchange interaction as compared to the

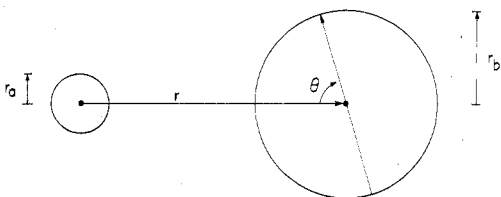


Figure 1. Schematic diagram of a two radical system with one radical exhibiting an angular dependence about a preferred axis in its properties.

role of translational diffusion. Also, it is found that asymmetric initial conditions can influence both CIDNP and CIDEP.

The details of solving the combined translational-rotational SLE are discussed in section II, and the results for CIDNP and CIDEP with isotropic initial conditions appear in sections III and IV, respectively. Effects due to anisotropic initial conditions are discussed in section V, while the conclusions appear in section VI.

## II. Method

We start with the following general form for the SLE:<sup>2</sup>

$$\frac{\partial \rho(\mathbf{r}, \Omega, t)}{\partial t} = -i\mathcal{H}^x(\mathbf{r}, \Omega)\rho(\mathbf{r}, \Omega, t) + \nabla_{\mathbf{r}} \cdot \mathbf{D} \nabla_{\mathbf{r}} \rho(\mathbf{r}, \Omega, t) + \nabla_{\Omega} \cdot \mathbf{R} \nabla_{\Omega} \rho(\mathbf{r}, \Omega, t) + \frac{1}{kT} \nabla_{\mathbf{r}} \cdot \mathbf{D} \{ \rho(\mathbf{r}, \Omega, t) [\nabla_{\mathbf{r}} U(\mathbf{r}, \Omega, t)] \} + \frac{1}{kT} \nabla_{\Omega} \cdot \mathbf{R} \{ \rho(\mathbf{r}, \Omega, t) [\nabla_{\Omega} U(\mathbf{r}, \Omega, t)] \} + K(\mathbf{r}, \Omega)\rho(\mathbf{r}, \Omega, t) + \mathcal{R}\rho(\mathbf{r}, \Omega, t) \quad (2.1)$$

where  $\rho(\mathbf{r}, \Omega, t)$  is the spin-density matrix,  $\mathcal{H}^x(\mathbf{r}, \Omega)$  is the Liouville operator associated with the spin Hamiltonian  $\mathcal{H}^x(\mathbf{r}, \Omega)$  (i.e.,  $A^x B \equiv [A, B]$ ),  $K(\mathbf{r}, \Omega)$  is a phenomenological spin-specific reaction operator,  $\mathcal{R}$  is the spatially independent part of the relaxation matrix,  $\mathbf{D}$  is the relative translational diffusion tensor,  $\mathbf{R}$  is the rotational diffusion tensor, and  $U(\mathbf{r}, \Omega)$  is the potential energy affecting the rotational and relative translational diffusion. For convenience, we are considering in eq 2.1 a relatively simple radical pair with each radical containing an unpaired electron. This pair is represented in Figure 1 and is comprised of a radical a, with spherically symmetric properties, whose center is chosen as the origin of the coordinate system within which the relative translational motion will be represented. The other radical b, with orientation specified by Euler angles,  $\Omega$ , and diffusion tensor,  $\mathbf{R}$ , will now, for simplicity, be assumed to have a single preferred axis  $\vec{e}$ , so that the single angle,  $\theta$ , as seen in Figure 1 is then sufficient to account for the relevant orientation-dependent interactions of the radical pair. This angle  $\theta$  is the angle between  $\vec{e}$  and the internuclear vector  $\vec{r}$ , which is the axis that connects the two radical centers. We shall also let  $U(\vec{r}, \Omega) = U(r)$  where  $r = |\vec{r}|$ ,  $\mathbf{D} \rightarrow D\mathbf{I}$ ,  $\mathbf{R} \rightarrow R\mathbf{I}$  for simplicity. We therefore simplify eq 2.1 by rewriting it [with  $\rho(\mathbf{r}, t) \rightarrow \rho(r, \theta, t)$  by integrating over the other "irrelevant" independent variables] as

$$\frac{\partial \rho(r, \theta, t)}{\partial t} = -i\mathcal{H}^x(r, \theta)\rho(r, \theta) + \frac{D}{r^2} \frac{\partial}{\partial r} \left( r^2 \frac{\partial \rho(r, \theta, t)}{\partial r} \right) + \frac{(D/r^2 + R)}{\sin \theta} \frac{\partial}{\partial \theta} \left( \sin \theta \frac{\partial \rho(r, \theta, t)}{\partial \theta} \right) + \frac{1}{kT} \left[ \frac{D}{r^2} \frac{\partial}{\partial r} \left( r^2 \rho(r, \theta, t) \frac{\partial U(r)}{\partial r} \right) + K(r, \theta)\rho(r, \theta, t) + \mathcal{R}\rho(r, \theta, t) \right] \quad (2.2)$$

The coefficient  $(D/r^2 + R)$  of the term involving  $\theta$  derivatives arises because the variation in  $\theta$  can come about by the independent effects of the translational motion of the two particles, hence the  $D/r^2$  term (cf. eq 2.5–2.7 of ref 2a),

and by rotation of the radical b, hence the  $R$  term. The fact that these two terms are simply additive is not immediately obvious, but a careful derivation of this result is given in Appendix A. (The more general case where both radicals exhibit anisotropic properties is also considered there.) We shall further simplify eq 2.2 by choosing  $U(r, \theta) = 0$  for  $r > d$  and  $U(d, \theta) = \infty$  (where  $d = r_a + r_b$  is the distance of closest approach and is assumed to be orientation independent). This latter condition is well described by a reflecting wall inner boundary condition. Spin-lattice relaxation effects will be neglected, since they may usually be included at a later stage in the analysis by using the two time scale approach of Pedersen and Freed<sup>2</sup> that takes advantage of the relatively rapid time scale for the evolution of CIDN(E)P.

Equation 2.2 also includes the isotropic translational and rotational diffusion coefficients,  $D$  and  $R$ . These may be defined from the Stokes-Einstein relations in terms of the hydrodynamic radii of the two radicals. Thus

$$D = \frac{kT}{6\pi\eta} \left( \frac{1}{r_a} + \frac{1}{r_b} \right) \quad (2.3)$$

with  $D = D_a + D_b$ , and

$$R = \frac{kT}{8\pi\eta r_b^3 \kappa} \quad (2.4a)$$

where  $\kappa$  is a correction factor, which, if less than unity, allows for the "rotational slip" of molecule b. A dimensionless ratio of interest then is

$$Rd^2/D = 3r_a d / 4\kappa r_b^2 \quad (2.4b)$$

We shall also use as the form of the spin specific reaction operator

$$K(r, \theta)\rho(r, \theta, t) = -k(r, \theta)|S\rangle \rho_{SS}(r, \theta, t) \langle S| \quad (2.5)$$

where  $\rho_{SS}(r, \theta, t)$  is the singlet-singlet diagonal density matrix element, while  $|S\rangle$  and  $\langle S|$  represent the singlet state ket and bra vectors. In our specific model we use

$$k(r, \theta) = \left[ k_0 + k_1 \left( \frac{1}{2} + \frac{1}{2} \cos \theta \right) \right] [\delta(r - d)] \quad (2.6)$$

which, together with eq 2.5, allows for an angular dependent reactivity of radicals which come in contact in the singlet state. The particular choice of  $k(r, \theta)$  is continuous in  $\theta$ . Salikhov<sup>6</sup> considered a discrete case [i.e.,  $k(r, \theta) = \text{constant}$  for  $\theta \leq \pi/2$  and  $k(r, \theta) = 0$  for  $\theta > \pi/2$ ], and we shall point out the similarities in our findings for the spin-independent reactivities.

The quantum mechanical superoperator,  $\mathcal{H}^x(r, \theta)$ , is now separated into its constant and spatially dependent parts:

$$\mathcal{H}^x(r, \theta) = \mathcal{H}_0^x + \mathcal{H}_J^x(r, \theta) \quad (2.7)$$

where

$$\mathcal{H}_J^x(r, \theta) = J(r, \theta) \left( \frac{1}{2} \mathbf{1} + 2\mathbf{S}_a \cdot \mathbf{S}_b \right) \quad (2.8)$$

and, by analogy to eq 2.6, we let

$$J(r, \theta) = \left[ J_0 + J_1 \left( \frac{1}{2} + \frac{1}{2} \cos \theta \right) \right] e^{-\lambda(r-d)} \quad (2.9a)$$

As usual<sup>2</sup> we define

$$r_{\text{ex}} \equiv 5 \ln 10 / \lambda \quad (2.9b)$$

so that  $r_{\text{ex}}$  is a measure of the range of the exchange interaction in radial space. This "exchange distance" will also be chosen to be independent of  $\theta$  for simplicity.

For high-field cases<sup>5,6</sup> we only need to consider the density matrix elements,  $\rho_\alpha(r, \theta, t)$  where  $\alpha = \text{SS}, \text{ST}_0, \text{T}_0\text{S},$  and  $\text{T}_0\text{T}_0$ . S and  $\text{T}_0$  here refer to the singlet (S) or triplet ( $\text{T}_0, m_s = 0$ ) electronic spin states. We can now consider these quantities,  $\rho_\alpha(r, \theta, t)$ , as elements of a vector,  $\rho(r, \theta, t)$ , which obeys a matrix equation of motion derivable from eq 2.2 by taking the  $\langle \alpha |, |\beta \rangle$  matrix elements of the spin-dependent operators. The elements of these matrices will then be denoted by, e.g.,  $\mathcal{H}^x(r, \theta)_{\alpha, \beta}$  and  $K(r, \theta)_{\alpha, \beta}$ .

Further simplification of eq 2.2 can be attained by first the change of variable  $\tilde{\rho}(r, \theta, t) = r\rho(r, \theta, t)$  and then multiplication of both sides of the equation by the scaling factor  $d^2/D$ . This enables us to reduce all the quantities to their dimensionless forms:  $y \equiv r/d, q \equiv Qd^2/D, y_{\text{ex}} \equiv r_{\text{ex}}/d, j_0 \equiv J_1d^2/D, \kappa \equiv k_0d^2/D, \kappa_1 \equiv k_1d^2/D,$  and  $\tau \equiv tD/d^2$ . Usually it is sufficient to solve for CIDN(E)P observables in the  $\tau \rightarrow \infty$  limit (but see ref 8 relating to two-dimensional systems). It is easiest, for computational reasons, to Laplace transform eq 2.2, employing the variable

$$\hat{\rho}(y, \theta, \sigma) \equiv \int_0^\infty e^{-\sigma\tau} \tilde{\rho}(y, \theta, \tau) d\tau \quad (2.10)$$

and to obtain the  $\tau \rightarrow \infty$  limit by solving for the results for  $\sigma \rightarrow 0$ . It has been found that a finite but small value for  $\sigma < 10^{-10}$  suffices.<sup>2,7,8</sup>

These modifications and the assumptions of our model allow us to rewrite eq 2.2 as

$$\sigma \hat{\rho}(y, \theta, \sigma) - \tilde{\rho}(y, \theta, 0) = -i[\mathcal{H}^x(y, \theta)d^2/D]\hat{\rho}(y, \theta, \sigma) + \frac{\partial^2 \hat{\rho}(y, \theta, \sigma)}{\partial y^2} + \frac{(1/y^2 + Rd^2/D)}{\sin \theta} \frac{\partial}{\partial \theta} \left( \sin \theta \frac{\partial \hat{\rho}(y, \theta, \sigma)}{\partial \theta} \right) + [K(y, \theta)d^2/D]\hat{\rho}(y, \theta, \sigma) \quad (2.11)$$

where  $\mathcal{H}^x(y, \theta)d^2/D$  in eq 2.11 is a function of  $q, j_0,$  and  $j_1$ . Using eq 2.7–2.9 we can write for  $\mathcal{H}_0^x$

$$\mathcal{H}_0^x d^2/D = \begin{pmatrix} \text{SS} & \text{ST}_0 & \text{T}_0\text{S} & \text{T}_0\text{T}_0 \\ 0 & -q & q & 0 \\ -q & 0 & 0 & q \\ q & 0 & 0 & -q \\ 0 & q & -q & 0 \end{pmatrix} \quad (2.12)$$

We now define

$$j'(y) \equiv (2j_0 + j_1)e^{-\lambda d(y-1)} \quad (2.13a)$$

$$j''(y, \theta) \equiv (j_1 \cos \theta)e^{-\lambda d(y-1)} \quad (2.13b)$$

and we find

$$[\mathcal{H}^x(y, \theta)d^2/D]_{\text{ST}_0\text{ST}_0} = -[\mathcal{H}^x(y, \theta)d^2/D]_{\text{T}_0\text{S}, \text{T}_0\text{S}} = j'(y) + j''(y, \theta) \quad (2.14a)$$

with all other

$$[\mathcal{H}^x(y, \theta)d^2/D]_{\alpha, \beta} = 0 \quad (2.14b)$$

The chemical reactivity of the radicals enters eq 2.11 through eq 2.5 and 2.6, such that the only nonzero term is

$$[K(y, \theta)d^2/D]_{\text{SS}, \text{SS}} = \kappa'(y) + \kappa''(y, \theta) \quad (2.15a)$$

where we have defined

$$\kappa'(y) \equiv (\kappa_0 + \frac{1}{2}\kappa_1)\delta(y-1) \quad (2.15b)$$

$$\kappa''(y, \theta) \equiv \frac{1}{2}\kappa_1(\cos \theta)\delta(y-1) \quad (2.15c)$$

We now expand the  $\hat{\rho}_\alpha(y, \theta)$  in a series of zero rank spherical harmonics,  $Y_L^0(\theta, \varphi)$ , according to

$$\hat{\rho}_\alpha(y, \theta, \sigma) = \sum_{L=0}^{\infty} \hat{\rho}_\alpha^{(L)}(y, \sigma) Y_L^0(\theta, \varphi) \quad \text{for all } \alpha \quad (2.16)$$

This expansion can usually be truncated<sup>9</sup> at some value of  $L = L_{\text{max}}$  such that convergence has been obtained. Thus we write

$$\hat{\rho}_\alpha(y, \theta, \sigma) \approx \sum_{L=0}^{L_{\text{max}}} \hat{\rho}_\alpha^{(L)}(y, \sigma) Y_L^0(\theta, \varphi) \quad \text{for all } \alpha \quad (2.17)$$

and perform test calculations to show that the residual error created by this truncation is negligible. This simplifies the analysis of eq 2.11 because the spherical harmonics are the orthonormal eigenfunctions of the rotational diffusion operator, with eigenvalues equal to  $L(L+1)$  (cf. Appendix A). This feature can be exploited by substituting  $\hat{\rho}(y, \theta, \sigma)$  formed by eq 2.17 into eq 2.11. Subsequent multiplication by  $Y_L^0(\theta)$  and integration over all allowed values of  $\theta, 0 \leq \theta \leq \pi,$  and  $\varphi, 0 \leq \varphi \leq 2\pi,$  yields the intermediate result

$$\sigma \hat{\rho}^{(L)}(y, \sigma) - \tilde{\rho}^{(L)}(y, 0) = i\mathcal{H}_0^x(d^2/D)\hat{\rho}^{(L)}(y, \sigma) + \frac{\partial^2 \hat{\rho}^{(L)}(y, \sigma)}{\partial y^2} + \left( \frac{1}{y^2} + \frac{Rd^2}{D} \right) L(L+1)\hat{\rho}^{(L)}(y, \sigma) + \sum_{L'=0}^{L_{\text{max}}} \hat{\rho}^{(L')}(y, \sigma) \left\{ \int_0^\pi Y_{L'}^0 K(y, \theta) Y_L^0 \sin \theta d\theta - i(d^2/D) \int_0^\pi Y_{L'}^0 \mathcal{H}^x(y, \theta) Y_L^0 \sin \theta d\theta \right\} \quad (2.18)$$

The integrals containing  $K(y, \theta)$  and  $\mathcal{H}^x(y, \theta)$  can be solved by noting<sup>10</sup> (see also the Appendix):

$$\int_0^{2\pi} \int_0^\pi Y_{L'}^0(\theta, \varphi) (\cos \theta) Y_L^0(\theta, \varphi) \sin \theta d\theta d\varphi = -L'/[(2L'-1)(2L'+1)]^{1/2} \equiv L'^+ \quad \text{for } L' = L-1 \\ = -(L+1)/[(2L+1)(2L+3)]^{1/2} \equiv L'^- \quad \text{for } L' = L+1 \quad (2.19a)$$

and the orthonormality relation

$$\int_0^{2\pi} \int_0^\pi Y_{L'}^0(\theta, \varphi) Y_L^0(\theta, \varphi) \sin \theta d\theta d\varphi = \delta_{L'L} \quad (2.19b)$$

with  $\delta_{L'L}$  the Kronecker delta.

We observe that the  $\theta$ -independent terms in eq 2.18 may couple coefficients (i.e.,  $\hat{\rho}_\alpha^{(L)}(y, \sigma)$ ) for different values of  $\alpha$  but with identical  $L$  indices. The  $\theta$ -dependent terms couple coefficients of the same  $\alpha$  but the  $L$  indices will be different. This is because the  $\theta$ -dependent terms of eq 2.14 and 2.15 are diagonal in the spin basis we are using.

The  $y$  dependence of eq 2.18 is treated by the method of finite differences (FD), where all quantities will be specified at discrete nodes in space. These nodes (connecting concentric shells of infinitesimal thickness) will be fixed at distances  $y_l$  where  $1 \leq l \leq N$ . The  $y_l$  are separated according to the geometrically increasing nodal separation scheme of Zientara and Freed:<sup>7a</sup>

$$y_l = 1 + \sum_{m=1}^{l-1} h^{(m)} \quad \text{for } l > 1 \quad (2.20a)$$

$$y_1 = 1 \quad (2.20b)$$

where

$$h^{(1)} \equiv \Delta_1 \quad (2.21a)$$

$$h^{(m)} \equiv \Delta_1(\Delta_0)^{m-1} \quad (2.21b)$$

Thus, all the nodal separations are determined by specifying just  $\Delta_1$  and  $\Delta_0$ . The transition matrix,  $\mathbf{W}$ , and volume factors  $\mathbf{V}$  resulting from the particular choice of eq 2.20 and 2.21 have been given previously (cf. eq 2.5–2.8 of ref 7a). These represent the FD analogues of the  $\partial^2/\partial y^2$  and  $y dy$  differential forms. Also, the coefficients,  $\hat{\rho}_\alpha^{(L)}(y, \sigma)$ ,

then are only known at the given set of nodes,  $\hat{\rho}_\alpha^{(L)}(l, \sigma) \equiv \hat{\rho}_\alpha^{(L)}(y, \sigma)$ . We may then construct a supervector containing the  $N$  sets of eq 2.18 written at all nodes

$$\hat{\rho}(\sigma) \equiv \begin{pmatrix} \hat{\rho}(1, \sigma) \\ \hat{\rho}(2, \sigma) \\ \vdots \\ \hat{\rho}(N, \sigma) \end{pmatrix} \quad (2.22)$$

with each subvector  $\hat{\rho}(l, \sigma)$  containing  $4(L_{\max} + 1)$  elements written in special sequence as

$$\rho(l, \sigma) \equiv \begin{pmatrix} \hat{\rho}_{SS}^{(0)}(l, \sigma) \\ \hat{\rho}_{ST_0}^{(0)}(l, \sigma) \\ \hat{\rho}_{T_0S}^{(0)}(l, \sigma) \\ \hat{\rho}_{T_0T_0}^{(0)}(l, \sigma) \\ \hat{\rho}_{SS}^{(1)}(l, \sigma) \\ \vdots \\ \hat{\rho}_{T_0T_0}^{L_{\max}}(l, \sigma) \end{pmatrix} \quad (2.23)$$

In a similar manner, operators on the right-hand side of eq 2.18 are replaced by a supermatrix structure,<sup>2,7</sup> such that a matrix equation results

$$\mathbf{A}\hat{\rho}(\sigma) = \tilde{\rho}(0) \quad (2.24)$$

where we have introduced  $\tilde{\rho}(0)$  as the initial condition. For example, if we wish an isotropic initial condition with the radicals in the triplet state and in contact then

$$\tilde{\rho}_{T_0T_0}^{(0)}(1, \tau=0) = [V(1)(4\pi)^{1/2}]^{-1} \quad (2.25)$$

where the numerical factor on the right-hand side consists of an angular normalization term and the FD volume factor,  $V(1)$ , associated with the first node. The structure of the supermatrix  $\mathbf{A}$  follows from past discussion. The translational diffusion part of  $\mathbf{A}$  is created from the elements of  $\mathbf{W}$ ; the  $L$ -independent quantum couplings result from eq 2.12, 2.13a, and 2.15b; the  $L$ -dependent couplings result from eq 2.13b and 2.15c; and rotational diffusion enters via the term  $(1/y^2 + Rd^2/D)L(L+1)$ . The construction of the partitioned  $\mathbf{A}$  is discussed in detail in Appendix B.

The calculation of  $\hat{\rho}(\sigma)$  was performed by Gaussian elimination with partial pivoting on a PDP 11/34 mini-computer. Once  $\hat{\rho}(\sigma)$  is calculated, we may obtain the relevant CIDN(E)P quantities from

$$\mathcal{P} = \lim_{\sigma \rightarrow 0} \sigma(4\pi)^{1/2} \int_1^\infty \int_0^{2\pi} \int_0^\pi [\hat{\rho}_{SS}(y, \theta, \sigma) + \hat{\rho}_{T_0T_0}(y, \theta, \sigma)] y \sin \theta \, d\theta \, d\varphi \, dy \quad (2.26a)$$

$$\simeq \lim_{\sigma \rightarrow 0} \sigma(4\pi)^{1/2} \sum_{l=1}^N [\hat{\rho}_{SS}^{(0)}(l, \sigma) + \hat{\rho}_{T_0T_0}^{(0)}(l, \sigma)] V(l) \quad (2.26b)$$

where  $\mathcal{P}$  is the probability the radical pair have not reacted at  $t = \infty$ . Also

$$P_a^\infty = -2 \lim_{\sigma \rightarrow 0} \sigma \int_1^\infty \int_0^{2\pi} \int_0^\pi \text{Re} \hat{\rho}_{ST_0}(y, \theta, \sigma) y \sin \theta \, d\theta \, d\varphi \, dy \quad (2.27a)$$

$$\simeq -2 \lim_{\sigma \rightarrow 0} \sigma(4\pi)^{1/2} \sum_{l=1}^N \text{Re} \hat{\rho}_{ST_0}^{(0)}(l, \sigma) V(l) \quad (2.27b)$$

CIDNP enhancements are usually related to  $\mathcal{F} = 1 - \mathcal{P}$ , the nuclear-spin-state-specific yields. In turn,  $\mathcal{F}$  may be related to two more basic quantities,  $\Lambda$  and  $\mathcal{F}^*$ , by expressions given elsewhere.<sup>2,7</sup> These  $\mathcal{F}$  relations, however,

are no longer found to be exact in our study, because of the angular degree of freedom introduced into the problem. Specifically,  $\Lambda$  is the spin-independent probability that a pair of radicals initially in contact will eventually react. It depends upon the reactivity vs. the diffusion effects.  $\mathcal{F}^*$  represents the probability that a pair of radicals initially in the triplet state and in contact will eventually react in the singlet state given infinite reactivity of singlets.  $\mathcal{F}^*$  therefore is only a function of diffusion vs. spin-dependent quantum effects. It has been found<sup>2,7a</sup> in earlier numerical studies that  $\mathcal{F}^* \simeq 1/2q^{1/2}$  for  $0 < q < 1$  in three dimensions and with a very small logarithmic dependence on  $j_0$ . Thus, in a study of orientation-dependent effects on CIDNP, it is sufficient, since  $q$  has no angular dependence, to anticipate that it is mainly the reactive effects (which determine  $\Lambda$ ) that will modify the value of  $\mathcal{F}$  for  $Rd^2/D > 0$ . These matters are discussed in section III.

CIDEP effects are most often calculated from  $P_a^\infty$  ( $\kappa_0 = 0$ , triplet initial) and related to cases where  $\kappa_0 > 0$  via the formulas of Pedersen and Freed.<sup>2a</sup> These formulas are also no longer expected to hold rigorously, especially when there are orientation dependences in both the reactivity and the exchange interaction. We do not attempt to present a complete numerical study of these situations, but instead present some typical results in section IV.

### III. CIDNP

In this section we shall analyze the effects of orientation-dependent interactions on CIDNP. We assume in this section that there is initially an isotropic angular distribution of radicals (cf. section V where this assumption is lifted). This initial distribution adequately describes the case of random radical encounters in a liquid (as F pairs, or encountering radicals formed from different reactant molecules). It also applies to geminate radical processes where rotational diffusion sufficiently randomizes the radical-radical  $\theta$  distribution before any significant translational separation occurs. At the outset, we can observe from previous CIDNP studies<sup>1,11</sup> that experimental data from systems of highly nonspherical species appear to be adequately described by a theory assuming spherically symmetric interactions.<sup>1,2</sup> One might hypothesize that angular dependent effects largely lead to results that may be described in terms of the same fundamental parameters as for spherically symmetric interactions, but the actual values of these parameters are modified by the angular dependences. We shall explore this matter further in the analysis of our results.

We start by recalling that in the past theoretical discussions<sup>2,7,8</sup> several exact CIDNP relations were found which relate  $\mathcal{F}$  to the fundamental quantities  $\mathcal{F}^*$  and  $\Lambda$  (cf. eq 3.1-3.9 of ref 2a). Thus, once these two parameters are determined, one immediately obtains results for  $\mathcal{F}$  under a variety of initial spin conditions. The justification of such relations (cf. ref 2a) followed simply from (1) the fact that only two spin states (S and  $T_0$ ) were involved, and (2) the simple  $r$ -dependent diffusional model leading to simple physical interpretation of multiple reencounters leading to the "collision". Once there are more relevant diffusional degrees of freedom or more allowed quantum states, this analysis becomes less straightforward<sup>7a</sup> or altogether impossible. In our present study, while we still retain the simplicity of only two quantum states (S and  $T_0$ ), the addition of orientation-dependent effects leads to the expectation that no such exact relations will exist. Nevertheless, for the simple model we studied (i.e.,  $\cos \theta$  orientation dependence) we still found these relations a useful first approximation. We therefore discuss our results, as before, first in terms of  $\Lambda$  and of  $\mathcal{F}^*$ , and then we

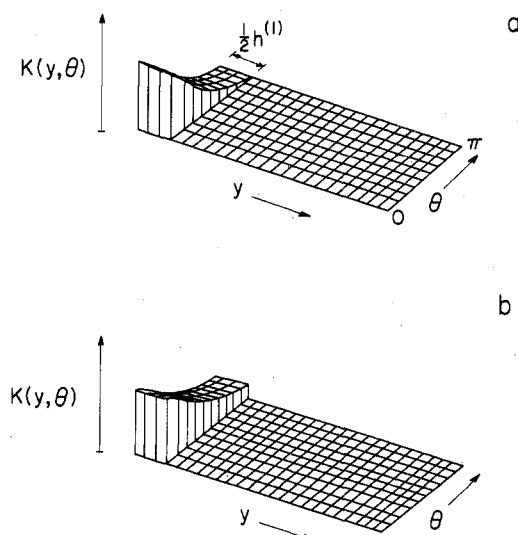


**Figure 2.**  $\kappa(y, \theta)$  for  $y \geq 1$ ,  $0 \leq \theta \leq \pi$  where  $\kappa(y, \theta) = \kappa_0 + \kappa_1 (1/2 + 1/2 \cos \theta)$  for  $1 \leq y \leq 1 + 1/2 h$  and  $\kappa(y, \theta) = 0$  elsewhere: (a) represents the case where  $\kappa_0 = 0$ ,  $\kappa_1 > 0$  and (b) represents  $\kappa(y, \theta)$  where  $\kappa_0, \kappa_1 > 1$ .

consider how effectively they may be used to approximate  $\mathcal{F}$ .

In our analysis, it is useful to define a dimensionless rotational correlation time (cf. eq 2.3 and 2.4) as

$$\tau_{R^*} \equiv \tau_R D / d^2 = \frac{1}{6} \left( \frac{R d^2}{D} \right)^{-1} = \frac{2 \kappa r_b^2}{9 d r_a} \quad (3.1a)$$

which we may then compare with a dimensionless characteristic time associated with a translational displacement of  $(\Delta y)^2$  in liquids given by<sup>12</sup>

$$\tau_T^*(\Delta y) \equiv \tau_T D / d^2 \equiv 1/6 (\Delta y)^2 \quad (3.1b)$$

Then a value of  $\tau_{R^*} = 1/3$ , for example, implies that the radicals would retain knowledge of the mutual orientation for the time required to separate a distance of about  $\sqrt{2}d$ . More precisely, however, the radical orientation relative to  $\vec{r}$  will decay with effective dimensionless time constant (cf. eq 2.18):

$$\tau_{R^* \text{ eff}}(y)^{-1} = \tau_{R^*}^{-1} + \tau_T^*(y)^{-1} \quad (3.2)$$

where  $\tau_T^*(y) = y^2/6$ .

We illustrate in Figure 2 typical forms for  $\kappa(y, \theta)$  which may be modeled by eq 2.6. Figure 2a corresponds to  $\kappa_0 = 0$ ,  $\kappa_1 > 0$ , while Figure 2b is for  $\kappa_0, \kappa_1 > 0$ . In both figures, following eq 2.6, the reaction is limited to the contact region extending  $h^{(1)}/2$  beyond the distance of closest approach (i.e., ranging from  $1 \leq y \leq 1 + h^{(1)}/2$ ). More sharply peaked reactivities may be modeled by including higher order terms in a Legendre polynomial expansion of  $\kappa(y, \theta)$  (cf. Appendix A). This may readily be incorporated into the present formalism, but it does lead to a larger value of  $L_{\text{max}}$  required for convergence, hence longer computations than were practical to perform in the present work.

The results obtained for  $\Lambda$  by using the forms for  $\kappa(y, \theta)$  illustrated in Figure 2 showed no peculiar effects except for the expected overall reduction in product yield due to the decrease in the reactive region (in  $\theta$  space) accessible to the radicals. Results for  $\Lambda$ , where  $\kappa_0 = 0$  and  $\kappa_1 > 0$  (cf. Figure 2a), are shown in Figure 3. We have determined that the results of Figure 3 are accurate to within 1% (by calculations which use  $L_{\text{max}} > 4$ ). One observes that the calculated results (given by the solid curve) do not deviate significantly from the results predicted by assuming

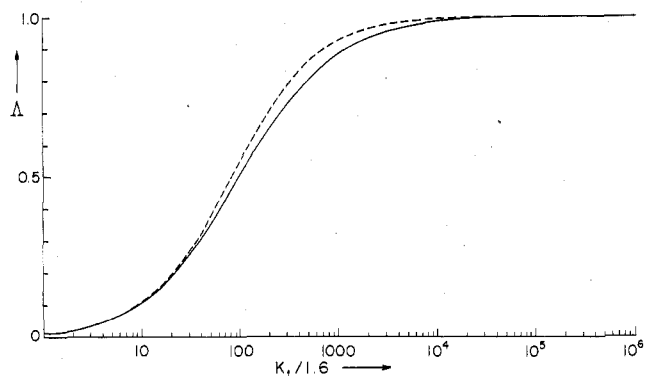


**Figure 3.**  $\Lambda$  vs.  $\kappa_1/1.6$  with  $\kappa_0 = 0$ . The solid curve exhibits numerical results calculated by using the additional input of  $\tau_{R^*} = 1/3$ ,  $q = j_0 = j_1 = 0$ ,  $\Delta_1 = 0.03125$ ,  $\Delta_0 = 1.225$ ,  $y_N = 2894$ ,  $N = 50$ ,  $L_{\text{max}} = 4$ , and an isotropic singlet initial condition. The dashed curve shows the theoretical values for  $\Lambda$  calculated from eq 3.3 and 3.4 and with  $\tau_1 = 0.015625$ .

spherical symmetry,<sup>2</sup> provided we introduce an effective reaction rate  $\kappa_{\text{eff}}$ , i.e.

$$\Lambda \simeq \frac{\kappa_{\text{eff}} \tau_1}{1 + \kappa_{\text{eff}} \tau_1} \quad (3.3)$$

where  $\tau_1 = h^{(1)}/2$  is a dimensionless lifetime of the interacting radical pair. Equations 2.15b and B.7b suggest the use of

$$\kappa_{\text{eff}} \simeq \kappa_0 + 1/2 \kappa_1 \quad (3.4)$$

in eq. 3.3. The dashed curve shown in Figure 3 is based on eq 3.3 and 3.4. For  $\tau_{R^*} = 1/3$ , as was used for the results shown in Figure 3, the simple form for  $\Lambda$  obtained by employing a  $\kappa_{\text{eff}}$  predicts the actual results with a maximum of less than 10% error.

When this same model was studied with different values of  $\tau_{R^*}$ , the effects of orientational relaxation upon reactivity were observed. In general, the values of  $\Lambda$  for a given value of  $\kappa_1$  will oscillate somewhat about some mean value as  $\tau_{R^*}$  is varied and all other parameters are kept constant. In the limit as  $\tau_{R^*} \rightarrow \infty$ , only the translational motion of the radicals yields orientational relaxation (cf. eq 3.2). In this limit, a uniform orientational distribution will be achieved by those radical pairs which separate and reencounter after a sufficiently long translational excursion.<sup>2,13</sup> The importance of such an effect is reduced (in three dimensions), because the reencounter probability from a separation  $r$  is  $t_f = r/d$ . Thus, those radical pairs which are not oriented favorably for reaction in their initial encounter will, in this limit, experience a reduced likelihood of reactivity from future encounters. We have indeed found an overall decrease in yield in this limit relative to the predictions of eq 3.3 and 3.4. As  $\tau_{R^*}$  is decreased from this limit, rotational diffusion becomes effective in randomizing the radical orientation without requiring translational excursions, so the effective reactivity is found to increase and reach an asymptotic maximum value as  $\tau_{R^* \text{ eff}}(y = 1)^{-1} \rightarrow \tau_{R^*}^{-1}$ . In this limit, the rotational diffusion causes many "rotational reencounters" leading to increased reactivity. Therefore we may expect that for  $\tau_{R^*} < 1$ , we may employ a relation like eq. 3.3 but with

$$\kappa_0 + \kappa_1 \geq \kappa_{\text{eff}} > \kappa_0 + 1/2 \kappa_1 \quad (3.5)$$

and this is exactly what is found from our numerical studies (where the actual  $\kappa_{\text{eff}}$  depends upon  $\kappa_0$  and  $\kappa_1$ ). Thus, in summary, it appears from our results that the simple form of eq 3.3 for  $\Lambda$  is an adequate approximation for orientation-dependent kinetics provided one utilizes a  $\kappa_{\text{eff}}$  as the effective first-order rate constant, where  $\kappa_{\text{eff}}$

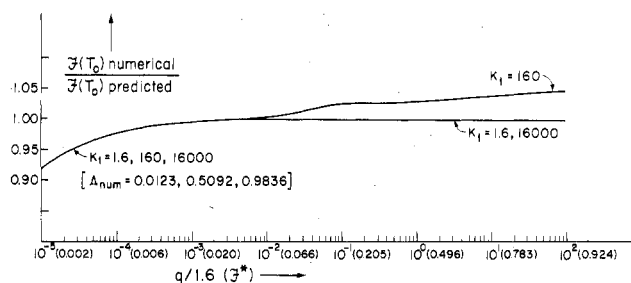


**Figure 4.** Ratio of numerical to predicted values of  $\mathcal{F}(T_0)$  vs.  $q$ , for  $\kappa_1 = 1.6, 160$ , and  $1.6 \times 10^4$ . Additional input includes  $\tau_R^* = 1/3$ ,  $\kappa_0 = j_0 = j_1 = 0$ ,  $\Delta_1 = 0.03125$ ,  $\Delta_0 = 1.225$ ,  $N = 50$ ,  $L_{\max} = 5$ , and anisotropic triplet initial condition. The predicted value for  $\mathcal{F}(T_0)$  is calculated from  $\mathcal{F}^*$  and  $\Lambda$  (exact numerical result) as shown by using Freed-Pedersen eq 3.9a (ref 2a).

$\leq \kappa_{\max}$  with  $\kappa_{\max} = \max[\kappa(y, \theta)]$ . Further,  $\kappa_{\text{eff}}$  increases as  $\tau_R^{*-1}$  increases.

Such ideas pertaining to the use of effective rate constants were discussed in previous studies.<sup>4,6</sup> Solc and Stockmayer<sup>4a</sup> point out that it is difficult or impossible to obtain knowledge of the orientation dependence of particle reactivity from the results of kinetic experiments. Such experiments only lead to an effective rate constant  $\kappa_{\text{eff}}$ .

Salikhov's approximate treatment<sup>6</sup> of rotational effects on recombination also yields the above conclusions.<sup>14</sup>

We now examine the implications of this result for CIDN(E)P observables (i.e., the spin-dependent effects), but first we must discuss orientation-dependent effects on  $\mathcal{F}^*$ . We have found from our results that  $\mathcal{F}^*$  is, to a good approximation, a function only of  $q$ , except for large values of  $j_0$  or  $j_1$  (i.e.,  $j_0, j_1 \gtrsim 10^3$ ). (For  $j_0 = j_1 = 0$  this statement is exactly true.) This result, for smaller  $j_0$  or  $j_1$  is not surprising, since  $\mathcal{F}^*$  is calculated in the limit that  $\Lambda \rightarrow \infty$ , or alternatively the limit that  $\kappa_{\text{eff}}\tau_1 \rightarrow \infty$ . In this limit, the orientational-dependent aspect of the reactivity should have no effect. The effect of a finite  $j(y, \theta)$  upon  $\mathcal{F}^*$ , with, for example,  $j_0 = 0, j_1 \gg 0$ , was similar to that found in previous studies on spherically symmetric interactions where  $j_0 \gg 0$  was used (cf. Table I of ref 5a and replace  $j_0$  by  $1/2j_1$ ). Thus, except for such cases where a large  $j(y, \theta)$  may produce a spatial region of significant extent in which S- $T_0$  transitions are suppressed, we expect that all the orientational effects will appear in the quantity  $\Lambda$ .

We now turn to the consideration of the relation between  $\mathcal{F}$  and  $\mathcal{F}^*$  and  $\Lambda$ . In particular we have examined the relation

$$\mathcal{F}(T_0) = \Lambda \mathcal{F}^* [1 + \mathcal{F}^*(1 - \Lambda)]^{-1} \quad (3.6)$$

which was found to be exact for the spherically symmetric case. We show in Figure 4 our results for the ratio  $\mathcal{F}(T_0)_{\text{num}}/\mathcal{F}(T_0)_{\text{pred}}$  where  $\mathcal{F}(T_0)_{\text{num}}$  is the exact numerical result and  $\mathcal{F}(T_0)_{\text{pred}}$  is the result predicted from eq 3.6 by using the exact numerical results for  $\Lambda$  and  $\mathcal{F}^*$ . Our results for  $q > 10^{-5}$  show that eq 3.6 is indeed a very good approximation, although it is not exact. For very small  $q \sim 10^{-5}$  where  $\mathcal{F}(T_0)_{\text{pred}} = \Lambda \mathcal{F}^*$ , it is a little larger than  $\mathcal{F}(T_0)_{\text{calcd}}$  and the deviation is independent of  $\Lambda$ . Thus, in this limit  $\mathcal{F}(T_0)$  is nearly, but not exactly, equal to the probability that triplets are converted to singlets ( $\mathcal{F}^*$ ) multiplied by the probability that singlets react. However, for  $q \gtrsim 10^{-2}$  the ratio for small  $\Lambda \sim 0.01$  and large  $\Lambda \sim 1$  converge to exactly unity, but that for  $\Lambda \sim 0.5$  is 1.02–1.05.

In general, for the limit  $\Lambda = 1$ , the exact limiting form must still apply:  $\mathcal{F}(S) \equiv \Lambda = 1$ ,  $\mathcal{F}(T_0) = \mathcal{F}^*$ , and  $\mathcal{F}(RI) = 1/2(1 + \mathcal{F}^*)$ . We show in Figure 5 the results for  $\mathcal{F}(T_0)_{\text{num}}/\mathcal{F}(T_0)_{\text{pred}}$  where  $\mathcal{F}(T_0)_{\text{pred}}$  is calculated from the exact  $\mathcal{F}^*$ , while  $\Lambda_{\text{eff}}$  was obtained by eq use of 3.3 and 3.4

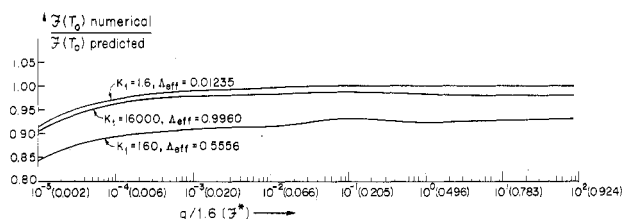


**Figure 5.** Ratio of numerical to predicted values of  $\mathcal{F}(T_0)$  vs.  $q$ , for  $\kappa_1 = 1.6, 160$ , and  $1.6 \times 10^4$ . Additional input includes  $\tau_R^* = 1/3$ ,  $\kappa_0 = j_0 = j_1 = 0$ ,  $\Delta_1 = 0.03125$ ,  $\Delta_0 = 1.225$ ,  $N = 50$ ,  $L_{\max} = 5$ , and an anisotropic initial condition. The predicted value of  $\mathcal{F}(T_0)$  is calculated from  $\mathcal{F}^*$  and  $\Lambda(\kappa_{\text{eff}})$  by using eq 3.3 and  $\kappa_{\text{eff}} = \kappa_0 + 1/2\kappa_1$ .

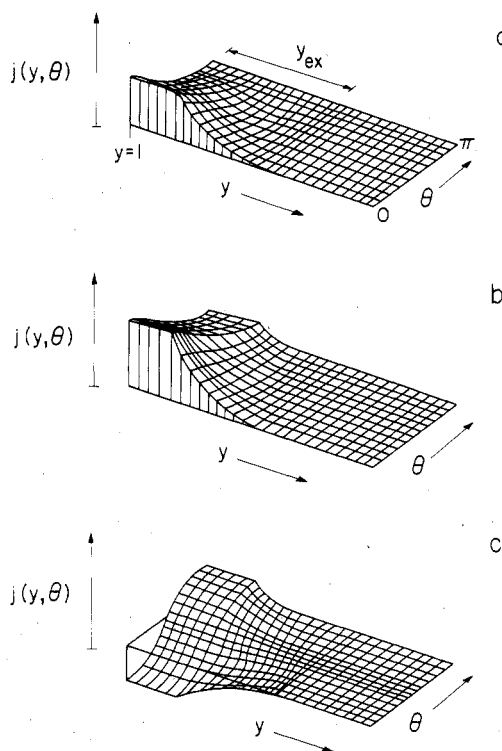


**Figure 6.**  $j(y, \theta)$  for  $y \geq 1, 0 \leq \theta \leq \pi$  where  $j(y, \theta) = [j_0 + j_1(1/2 + 1/2 \cos \theta)]e^{-\Lambda d(y-1)}$ : (a) is the case where  $j_0 \approx 0, j_1 > 0$ , (b) represents  $j_0 > 0, j_1 > 0$ , and (c) is the case where  $j(y, \theta)$  changes sign due to  $j_0 > 0, j_1 < 0$  but  $|j_1| > j_0$ .

(and  $\tau_R^* = 1/3$ ). Here the discrepancy is somewhat greater, but still the comparison is rather good. Again the greatest discrepancy appears for  $\Lambda \sim 0.5$ .

We thus conclude this section by noting that our model results indicate that the important CIDNP observable  $\mathcal{F}$  can be rather well estimated by the use of a theory for spherically symmetric interactions, and a  $\Lambda_{\text{eff}}$  which is a simple function of  $\kappa_{\text{eff}}\tau_1$  via eq 3.3. It is generally difficult to relate a  $\Lambda_{\text{eff}}$ , which may be determined by a (CIDNP) experiment, to the microscopic details of the molecular mechanism embodied in the parameters  $\kappa_{\text{eff}}$  and  $\tau_1$ .<sup>2</sup>

#### IV. CIDEP

In discussing our results on CIDEP polarizations we first consider the cases where  $\kappa_0 = \kappa_1 = 0$  (i.e., no reactivity) but  $j = j(y, \theta)$ . We consider only isotropic initial conditions in  $\theta$  in this section and defer to section V the discussion of effects of anisotropic initial conditions. Several cases of the variation of  $j(y, \theta)$  with  $y$  and  $\theta$ , which we consider, are represented pictorially in Figure 6. The example of Figure 6a (where  $j_0 = 0$  and  $j_1 > 1$ ) would correspond to a maximum exchange when  $\theta = 0$  with a minimum value at  $\theta = \pi$  of zero. This would crudely model an unpaired electron in a directed orbital on radical b. In Figure 4b this effect is less pronounced, since  $j_0 \neq 0$ , while in Figure 6c  $j(y, \theta)$

TABLE I: Variation of  $P_a^\infty \times 10^3$  with  $Rd^2/D^a$ 

$Rd^2/D$	$\tau_R^*$	I <sup>d</sup>	II <sup>e</sup>	III <sup>d</sup>	IV <sup>d</sup>
		$j_0 = 0$ $j_1 = 14.4$	$j_0 = 16$ $j_1 = 14.4$	$j_0 = 0$ $j_1 = 1600$	$j_0 = 16$ $j_1 = 1600$
0.050 <sup>b</sup>	3.33	98.4	54.5	33.4	34.5
0.055	3.03	90.7	55.1	27.4	27.4
0.50	0.33	87.4	55.4	27.0	26.8
0.55	0.303	65.8	55.4	25.3	25.6
1.0	0.167	105.5	55.2	28.3	27.9
1.1	0.152	93.3	55.0	29.1	29.1
5.0	0.033	118.3	56.1	27.1	27.1
5.5	0.030	106.3	55.2	27.7	27.7
50 <sup>c</sup>	0.0033	103.7	54.8	27.7	27.6
55	0.0030	102.3	54.7	27.6	27.5

<sup>a</sup> Finite difference numerical results for  $P_a^\infty \times 10^3$  found by using input as shown and  $q = 0.064$ ,  $y_{\text{ex}} = 1$ ,  $\kappa_0 = \kappa_1 = 0$ ,  $L_{\text{max}} = 6$ ,  $\Delta_I = 0.03125$ ,  $\Delta_0 = 1.225$ ,  $y_N = 2894$ ,  $N = 50$ , and an isotropic triplet initial condition. The value of  $y_{\text{ex}} = 1$  corresponds to a translational exchange lifetime of  $\tau_\lambda \approx 0.094$ . Results obtained by using  $L_{\text{max}} = 5$  show that the polarizations in this table represent numerically convergent values within about 1% of the actual value. <sup>b</sup>  $Rd^2/D = 0.050$  and  $\kappa = 1$  implies  $r_b \approx 16r_a$ , from eq 2.4b. <sup>c</sup>  $Rd^2/D = 50$  and  $\kappa = 1$  implies  $r_b \approx 1/6r_a$ . <sup>d</sup> Cf. Figure 4a. <sup>e</sup> Cf. Figure 4b.

changes sign as a function of  $\theta$  since  $j_0 > 0$  but  $j_1 < 0$  (but  $|j_1| > j_0$ ). This latter case is interesting theoretically and might conceivably be realized in practice.

Our results given below can be extended by the use of the relations

$$P_a^\infty(\kappa_0 = \kappa_1 = 0, q, -j_0, -j_1) = -P_a^\infty(\kappa_0 = \kappa_1 = 0, q, j_0, j_1) \quad (4.1)$$

for any initial condition, while

$$P_a^\infty(\kappa_0 = \kappa_1 = 0, q, j_0, j_1, \text{SI}) = -P_a^\infty(\kappa_0 = \kappa_1 = 0, q, j_0, j_1, \text{TI}) \quad (4.2)$$

where SI and TI refer to singlet or triplet initial conditions, respectively. Equations 4.1 and 4.2 follow from the symmetries of the SLE as previously noted.<sup>2</sup> However, the sign of  $P_a^\infty$  no longer follows from the simple rules used earlier<sup>2</sup> based upon the signs of  $q$  and  $j_0$ , unless (1)  $|j_1| < |j_0|$  if sign  $[j_0] = -\text{sign}[j_1]$ , or else (2) if sign  $[j_0] = \text{sign}[j_1]$ . The breakdown of any simple sign rules is especially true for the case of Figure 6c, as will be seen below.

We now consider the case of Figure 4a in somewhat more detail. When the radical pair are close enough that  $y < y_{\text{ex}}$  and  $|j_1| \gtrsim 1$ , it follows that for  $\theta < \pi/2$  the exchange interaction  $j(y, \theta)$  is appreciable; but for  $\theta > \pi/2$  it is very small. Thus, this is a situation where the "rotational encounter" mechanism can play an important role; i.e., the exchange interactions may be "turned on" or "turned off" merely by the rotational diffusion (and the orientation-dependent part of the translational diffusion, cf. eq 3.1). This will be in addition to (and in competition with) the effects of the "translational encounter" mechanism<sup>2,13</sup> which is the only process modulating  $j(y)$  for spherically symmetric (i.e.,  $y = 0$ ) exchange interactions. The case of Figure 4b is more nearly like the spherically symmetric case, so it is much less affected by the "rotational encounter" mechanism.

Typical results shown in Table I clearly exhibit the sensitivity of the polarizations to rotational reencounters. Case I of this table ( $j_0 = 0$ ,  $j_1 = 14.4$ ) corresponds to the situation of maximum, or near maximum, polarization for each value of  $\tau_R^*$ . The greatest sensitivity to rotational reencounters occurs for  $\tau_R^* \sim 1/6$ , in which region  $P_a^\infty$  exhibits an oscillatory variation with  $\tau_R^*$ . In this sensitive region, it must be that small increases or decreases in the number of rotational reencounters can significantly modify  $P_a^\infty$ . This is reasonable if we recall that a maximum in  $P_a^\infty$

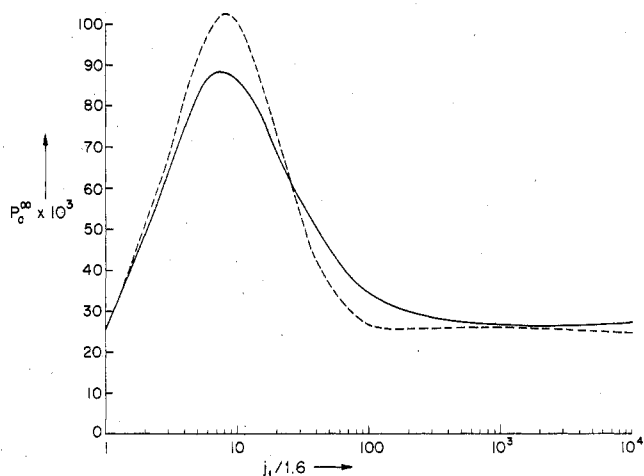


Figure 7.  $P_a^\infty \times 10^3$  vs.  $j_1/1.6$  with the additional input of  $j_0 = 0$ ,  $q = 0.064$ ,  $y_{\text{ex}} = 1$ ,  $\Delta_I = 0.03125$ ,  $\Delta_0 = 1.225$ ,  $y_N = 2894$ ,  $N = 50$ , and an anisotropic triplet initial condition. The solid curve exhibits the numerical results including rotational diffusion effects with  $\tau_R^* = 1/3$  and  $L_{\text{max}} = 4$ . The dashed curve shows numerical results excluding orientational effects, i.e.,  $\tau_R^{*-1} = 0$ ,  $L_{\text{max}} = 0$ .

vs.  $j(y, \theta)$  results from a competition between the polarizing mechanism (linear in  $j$ ) and the depolarizing (Heisenberg spin-exchange) mechanism (quadratic in  $j$ ), so shifts in the effective encounters can modulate the competing effects of these two processes. However, for large  $\tau_R^*$  the rotational diffusion is no longer very important (with the dominant reorientation of  $\theta$  due to the diffusion of  $\vec{r}$ ), while for very small  $\tau_R^*$  many rotational encounters take place before any translational diffusion occurs, and one has a single effective orientationally averaged exchange interaction,  $\overline{j(y, \theta)}$ .

If we recall that the (dimensionless) lifetime,  $\tau_\lambda^*$ , of the exchanging radical pair is

$$\tau_\lambda^* \approx \frac{1}{\lambda d} \left( 1 + \frac{1}{\lambda d} \right) \quad (4.3)$$

with  $\lambda$  defined in eq 2.9, then our results suggest that rotational reencounters will be important when  $\tau_R^* \lesssim \tau_\lambda$  (e.g., in Table I,  $\tau_\lambda \approx 0.1$ ).

The results in columns I and II of Table I may now be compared. Those of column II correspond to the case of Figure 4b (i.e.,  $j_0 = 16$ ;  $j_1 = 14.4$ ). Here we find there is no range of  $\theta$  where  $j(y \approx 1, \theta)$  is suppressed [i.e., there is no  $\theta$  for which  $j(y \approx 1, \theta) < q$ ]. In this case the predicted  $P_a^\infty$  are constant to within 2% even though  $\tau_R^*$  is varied over three orders of magnitude. Clearly, only the translational reencounter mechanism plays a significant role.

The results in columns III and IV of Table I, where  $j_1 = 1600$  and  $j_0 = 0$  and 16 respectively, are typical of results where asymptotic polarizations for large  $j(y, \theta)$  have been achieved. The existence of finite asymptotic  $P_a^\infty$  for large  $j_0 > 10^3$  is well known from previous work,<sup>2</sup> but these results in Table I as well as in Figure 7 demonstrate that, even for the case of Figure 6a, the same is true in the orientation-dependent case. Whether the asymptotic limit is achieved with a large  $j_0$  or  $j_1$  (or both),  $P_a^\infty$  is virtually the same. Furthermore, we find that varying  $\tau_R^*$  over three orders of magnitude has very little effect upon  $P_a^\infty$  (except for  $\tau_R^* > 3$ ). This is presumably because for such large values of  $j_1(1, \theta)$ , we have  $|j_1(1, \theta)| \gg q$  for most values of  $\theta$ , thus suppressing the importance of rotational reencounters, with reencounters via diffusion in  $\vec{r}$  required to generate the asymptotic values.

The results in Figure 7 illustrate how the asymptotic limit is achieved as  $j$  increases. We show an orientation-

TABLE II: CIDEP in the Presence of Asymmetric Chemical Reactivity<sup>a,b</sup>

exchange interaction input	$\kappa_1/\Lambda$	$10^3 P_a^\infty$ (s)	$10^3 P_a^\infty(T_0)$	$10^3 [P_a^\infty(\text{RI})/\mathcal{F}(\text{RI})]$
$\left. \begin{array}{l} j_0 = 0 \\ j_1 = 16 \\ (\mathcal{F}^* = 0.120, P_{a^{\infty}}^{\kappa=0}(T_0) \times 10^3 = 86.1) \end{array} \right\}$	1.6/0.012	-84.9(-85.1)	86.2(86.2)	108.0(86.1)
	160/0.509	-35.8(-44.7)	91.2(91.0)	103.2(86.1)
	$1.6 \times 10^{20}/1.0$	0.0(0.0)	95.0(96.4)	84.8(86.1)
$\left. \begin{array}{l} j_0 = 0 \\ j_1 = 1600 \\ (\mathcal{F}^* = 0.105, P_{a^{\infty}}^{\kappa=0}(T_0) \times 10^3 = 26.9) \end{array} \right\}$	1.6/0.012	-26.5(-26.6)	26.9(26.9)	31.3(26.9)
	160/0.509	-12.2(-14.0)	28.4(28.4)	31.1(26.9)
	$1.6 \times 10^{20}/1.0$	0.0(0.0)	29.6(29.7)	26.8(26.9)
$\left. \begin{array}{l} j_0 = 1600 \\ j_1 = 16000 \\ (\mathcal{F}^* = 0.101, P_{a^{\infty}}^{\kappa=0}(T_0) \times 10^3 = 26.7) \end{array} \right\}$	1.6/0.012	-25.7(-26.4)	26.8(26.8)	88.4(26.7)
	160/0.509	-4.2(-13.7)	27.9(28.0)	48.1(26.7)
	$1.6 \times 10^{20}/1.0$	0.0(0.0)	27.9(29.4)	25.4(26.7)

<sup>a</sup> The first results are the accurately calculated ones; the results in parentheses are predicted by using eq 4.5 (and its analogues, cf. ref 2a, eq 3.20-3.23) and the calculated values of  $\mathcal{F}^*$  and  $P_{a^{\infty}}^{\kappa=0}(T_0)$ . <sup>b</sup> Other values used are  $\kappa_0 = 0$ ,  $\gamma_{\text{ex}} = 1$ ,  $L_{\text{max}} = 5$ ,  $\tau_{\text{R}}^* = 1/3$ ,  $q = 0.064$ ,  $\Delta_{\text{I}} = 0.03125$ ,  $\Delta_0 = 1.225$ ,  $N = 50$ ,  $\gamma_{\text{N}} = 2894$ .

dependent case where  $j(y, \theta) = 1/2j_1(1 + \cos \theta)e^{-\lambda d(y-1)}$  and an orientation-independent case where  $j(y) = 1/2j_1e^{-\lambda(d-1)}$ . Both exhibit almost the same asymptotic limit, and nearly the same value of  $j_1(\text{max})$  (corresponding to the maximum in  $P_a^\infty$ ), while the  $P_{a^{\infty}}^{\text{max}}$  are within about 15% of each other. By varying  $\tau_{\text{R}}^*$ , one finds that  $P_{a^{\infty}}^{\text{max}}$  varies about  $\pm 50\%$  (for the solid curve) while  $j_1(\text{max})$  hardly changes. The peak widths are generally broader for the orientation-dependent models. Also  $P_{a^{\infty}}^{\text{max}}$  shifts to higher values of  $j$  as  $\gamma_{\text{ex}}$  decreases just as is the case for spherically symmetric interactions.<sup>2a</sup> The results typified by Figure 7 are indeed consistent with the qualitative predictions of Pedersen and Freed<sup>15</sup> for nonspherically symmetric cases.

Our results thus suggest that, for an exchange interaction of the form of eq 2.13a, the observed  $P_a^\infty$  may be adequately approximated by the predictions of the theory based upon spherically symmetric exchange interactions<sup>2</sup> if one uses an effective exchange interaction:

$$j_{\text{eff}}(y) \approx (j_0 + 1/2j_1)e^{-\lambda d(y-1)} \quad (4.4)$$

except in the region of  $P_{a^{\infty}}^{\text{max}}$  (cf. column I of Table I) where deviations of the order of a factor of 2 may occur.

We now turn to consideration of CIDEP in the presence of chemical reactions. The primary equation for this situation for spherically symmetric interactions (i.e.,  $j_1 = \kappa_1 = 0$ ) is<sup>2</sup>

$$P_a^\infty(\text{RI})/\mathcal{F}(\text{RI}) = P_{a^{\infty}}^{\kappa=0}(T_0) \quad (4.5)$$

However, we find that for anisotropic interactions eq 4.5 is no longer generally true. When, however, the reactivity is orientation dependent and  $|j(1, \theta)| \gtrsim 10^3$  and  $\Lambda \simeq 1$ , then eq 4.5 is very nearly obeyed. This can readily be understood, because the condition  $\Lambda \simeq 1$  implies that there is virtually complete depletion of all radicals within the reactive sphere, since the radical rotation-reaction process overcomes the effect of the reduction in the size of the reactive region. Then the polarization can develop as though the radicals present are initially all in the  $T_0$  state. Equation 4.5 is also very nearly obeyed if there is a spherically symmetric reactivity and  $|j(1, \theta)| \gtrsim 10^3$ .

However, deviations from eq 4.5 (as well as the other equations of Pedersen and Freed<sup>2</sup> relating  $P_a^\infty$  in the presence of reactivity to values in the absence of reactivity) will occur when there is an orientation-dependent reactivity and  $\Lambda < 1$ . Typical results are shown in Table II. In all cases we considered, the angular-dependent parts of  $j(y, \theta)$  and  $\kappa(y, \theta)$  were both centered about the same value of  $\theta$  as seems physically reasonable. Thus, from eq 2.6 and 2.9, it follows that the only way in which the "shapes" of  $j(y, \theta)$  and  $\kappa(y, \theta)$  vs.  $\theta$  may be different is in the relative weightings of  $j_0$  vs.  $j_1$  on the one hand and  $\kappa_0$  vs.  $\kappa_1$  on the other. We see from Table II that, when  $j_0 = \kappa_0 = 0$ , there

are indeed deviations from eq 4.4 but they are not very large. However, in the case that  $\kappa_0 = 0$  but  $j_0$  and  $j_1$  are both substantial, then deviations from eq 4.4 by more than a factor of 2 are found. We may explain these results as implying that when  $j$  and  $\kappa$  have the same orientational dependence, then they are both similarly affected by rotational reencounters as well as by translational reencounters, so the overall mechanism generating the polarization is similar to that from the reactive-independent process alone. Thus, large deviations are not to be expected in this case. On the other hand, when  $\kappa$  is more highly orientation dependent than  $j$  (and  $\Lambda < 1$ ), then there is a highly nonuniform (spin-dependent) depletion of the interacting radical pairs, so that there is considerable variation of the nature of the radical pairs (viz. their spin states) over the broader range of values of  $\theta$  which can effectively engage in exchange. Such effects might well be enhanced by the use of more sharply peaked orientation-dependent  $\kappa(y, \theta)$  than we have used in our model calculations.

Paul, in his recent CIDEP study,<sup>16</sup> has found that his results are consistently about four times greater than predicted by a spherically symmetric theory.<sup>2</sup> In his analysis he considers  $P_{a^{\infty}}^{\text{asympt}}$ . He suggests that this might be due to anisotropic exchange effects. Our results in this section do not, however, support this point of view. As we have just shown, it is only when  $\kappa$  is more highly orientation dependent than  $j$  that there are significant deviations noted from spherically symmetric theory. However, Paul has found from a study of both geminate recombination and from random encounter recombination that eq 4.5 is obeyed even though  $P_a^\infty(\text{RI})/\mathcal{F}(\text{RI})$  and  $P_{a^{\infty}}^{\kappa=0}(T_0)$  are both about a factor of 4 large. Our results in Table II show that when  $P_a^\infty(\text{RI})/\mathcal{F}(\text{RI})$  is found to be significantly larger due to anisotropy, then  $P_{a^{\infty}}^{\kappa=0}(T_0)$  is still in very good agreement with a spherically symmetric theory, so that eq 4.5 is seriously violated. One must, therefore, look to other model-dependent features noted by Paul<sup>16</sup> and by Pedersen-Freed<sup>2</sup> which can influence  $P_a^\infty$  and not violate eq 4.5. On the other hand, it is possible that the importance of orientation-dependent effects may show up in future experiments precisely in that eq 4.5 is violated.

Situations that cannot be approximated by the use of a spherically symmetric theory are depicted in Figure 6c. In this case  $j(y, \theta)$  will change sign with  $\theta$ . Several examples are illustrated in Figure 8 with the resulting polarizations. Although the exchange interaction has in each case a large enough value that would normally imply a result close to the asymptotic polarization (i.e.,  $P_a^\infty = 27.0$  with  $|j_0| = 1600$ ,  $|j_1| = 1600$ , and other values as for Figure 8), it is evident from Figure 8 that these results correspond more closely to what one would expect from a simple spherically sym-

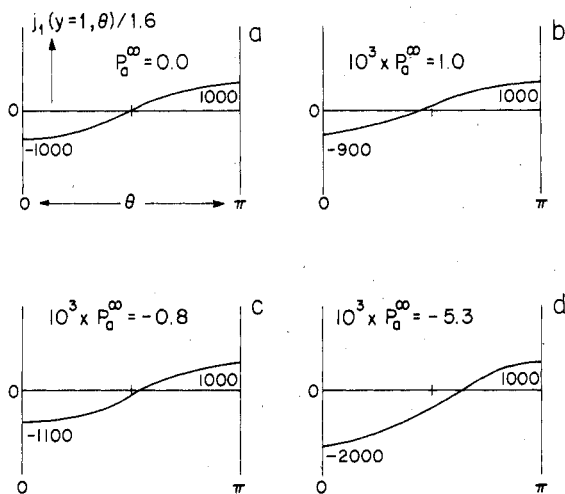


**Figure 8.**  $j_1(y, \theta)/1.6$  vs.  $\theta$  with the numerical result for  $P_a^\infty$  associated with each example.  $\theta$  varies from 0 to  $\pi$  with values of  $j(y=1, \theta=0) = j_0 + j_1$  and  $j(y=1, \theta=\pi) = j_0$  noted on each diagram. Additional input includes  $\tau_R^* = 1/3$ ,  $q = 0.064$ ,  $y_{ex} = 1$ ,  $j_0 = 1600$ ,  $\Delta_1 = 0.03125$ ,  $\Delta_0 = 1.225$ ,  $N = 50$ ,  $y_N = 2894$ ,  $L_{max} = 6$ , and an isotropic triplet initial condition. Values of  $j_1$  used are: (a)  $-3200$ ; (b)  $-3040$ ; (c)  $-3360$ ; and (d)  $-4800$ .

metric model with an angular average of the exchange interaction. This is most dramatically revealed by Figure 8a, where the exchange interaction is antisymmetric about  $\theta = \pi/2$  and yields no polarization even though  $|j(y, \theta \neq \pi/2)| \gg q$ . It is not obvious whether real examples of this case may actually be found.

### V. Anisotropic Initial Conditions

One might expect that recently formed geminate radical pairs will retain some memory of their initial relative orientation, and, if the interactions leading to CIDN(E)P are anisotropic, then this initial orientation should affect the polarizations. On the other hand, radical pairs formed from random encounters (i.e., F pairs) will be accurately described by an isotropic initial distribution, since this follows from spatial isotropy.<sup>17</sup>

We now consider effects of anisotropic initial conditions on CIDN(E)P observables. We choose as a particular anisotropic initial condition to replace eq 2.25 by

$$\tilde{\rho}_\alpha(1, \theta, \tau=0) = \frac{1}{(4\pi)}(1 + \cos \theta) \frac{1}{V(1)} \quad (5.1)$$

where  $\alpha$  corresponds to the particular nonzero spin matrix element(s). We may write for the expansion coefficients (cf. eq 2.16)

$$\tilde{\rho}_{ii}^0(1, \theta, \tau=0) = \frac{1}{(4\pi)^{1/2}V(1)} \quad (5.2a)$$

$$\tilde{\rho}_{ii}^1(1, \theta, \tau=0) = \frac{1}{(12\pi)^{1/2}V(1)} \quad (5.2b)$$

$$\tilde{\rho}_{ii}^{(L)}(1, \theta, \tau=0) = 0 \quad \text{for } L > 1 \quad (5.2c)$$

This corresponds to having as the most likely initial orientation:  $\theta \approx 0$ . More sharply peaked initial distributions may be achieved by including higher order spherical harmonics in eq 5.1, but they will require a larger value of  $L_{max}$  to achieve convergence.

We compare in Table III results for  $\Lambda$  obtained by using eq 5.2 with those obtained by using eq 2.25 for several values of  $\kappa_0$ ,  $\kappa_1$ , and  $\tau_R^*$ , but with  $\tau_I = 0.0156$ . We find that, in general, the two sets of results exhibit differences, which are small. We can explain this result simply as reflecting the fact that the anisotropic initial condition "relaxes" to an isotropic distribution in a time  $\tau_{R^*eff}(1)$  given by eq 3.2.

**TABLE III: Variations in  $\Lambda$  Due to an Anisotropic Initial Condition<sup>a</sup>**

$\kappa_0/\kappa_1$	$\tau_R^*$	0.033	0.33	3.33
	$\tau_{R^*eff}$	0.033	1/9	1/6.3
0/16		0.12(0.11)	0.08(0.11)	0.11(0.11)
0/160		0.65(0.59)	0.43(0.51)	0.53(0.55)
16/16		0.28(0.27)	0.25(0.27)	0.27(0.27)

<sup>a</sup> Finite difference numerical results for  $\Lambda$  from an anisotropic singlet initial condition, favoring a concentration of radical pairs with  $\theta \leq \pi/2$ , are listed first followed by the results where an isotropic initial condition is utilized. Additional input includes  $q = j_0 = j_1 = 0$ ,  $\Delta_1 = 0.03125$ ,  $\Delta_0 = 1.225$ ,  $N = 50$ ,  $y_N = 2894$ , and  $L_{max} = 6$ . Note  $\tau_I = 0.015625$ .

**TABLE IV: Variations in  $P_a^\infty$  Due to an Anisotropic Initial Condition**

Part A. No Chemical Reaction Allowed, <sup>a</sup>			
Results for $P_a^\infty$ ( $\kappa_0 = \kappa_1 = 0, T_0$ ) $\times 10^3$			
$j_0/j_1$	$\tau_R^*$	0.033	0.33
	$Rd^2/D$	5.0	0.5
0/16		100.4(118.2)	64.1(86.1)
0/1600		26.6(27.1)	23.1(27.0)
16/16		51.3(54.9)	81.9(54.2)
16/1600		26.6(27.1)	21.3(26.8)
Part B. Reaction Included, <sup>b</sup>			
Results for $P_a^\infty$ ( $\kappa_0, \kappa_1 \neq 0, T_0$ ) $\times 10^3$			
$\kappa_1/\kappa_0$	$\tau_R^*$	0.033	0.33
	$Rd^2/D$	5.0	0.5
0/16		26.9(27.4)	23.9(27.2)
0/160		28.2(28.7)	26.0(28.4)
16/16		27.3(27.8)	24.5(27.7)
Part C. Reaction Included, <sup>b</sup>			
Results for $P_a^\infty$ ( $\kappa_0, \kappa_1 \neq 0, S$ ) $\times 10^3$			
$\kappa_0/\kappa_1$	$\tau_R^*$	0.033	0.33
	$Rd^2/D$	5.0	0.5
0/16		-23.5(-24.3)	-21.3(-23.9)
0/160		-9.2(-11.5)	-12.3(-12.5)
16/16		-19.4(-20.2)	-17.8(-19.9)

<sup>a</sup> Finite difference numerical results for  $P_a^\infty$  from an anisotropic triplet initial condition, favoring radical pairs oriented with  $\theta \leq \pi/2$ , are listed first followed by the results obtained by using an isotropic triplet initial condition. Additional input includes  $q = 0.064$ ,  $y_{ex} = 1$ ,  $\Delta_1 = 0.03125$ ,  $\Delta_0 = 1.225$ ,  $N = 50$ ,  $y_N = 2894$ , and  $L_{max} = 6$ . Numerical convergence of these results was checked by noting that the change in the results obtained by using  $L_{max} = 6$  was  $< 5\%$  from the  $L_{max} = 5$  results. <sup>b</sup> Same method of presentation of numerical  $P_a^\infty$  results except that  $j_0 = 0$ ,  $j_1 = 1600$ , and other input parameters as in part A were used with only  $\kappa_0$ ,  $\kappa_1$ , and  $Rd^2/D$  varying to exhibit reactive effects.

This is typically short enough (even in the limit  $\tau_{R^*eff}(1) \rightarrow \tau_T^*(1)$ ) that there are sufficient translational encounters, after the orientations have been randomized, to yield comparable results for the two cases. There are enhanced reactivities when  $\tau_R^*$  is very short, presumably due to the enhanced effects of the initial condition on the first encounter followed by randomization of orientations on subsequent encounters; while as  $\tau_{R^*eff} \rightarrow \tau_T^*(1)$  the results for the two cases become virtually identical.

We show typical results for CIDEP in Table IV. Again we compared results obtained with eq 5.2 vs. those obtained with eq 2.25. There is, for no reactivity, in most cases a decrease in  $P_a^\infty$  due to the anisotropic initial condition, but again the effects are not very large, undoubtedly for similar reasons to those discussed for  $\Lambda$ . The observed decrease we may interpret as due to having a large fraction of radical pairs oriented such that initially  $|j(y, \theta)| > q$ , so

the radicals must reorient, or else separate, before the usual polarization process may begin by  $q$  mixing. However, for an isotropic initial distribution, a greater fraction of the radical pairs are oriented such that  $|j(y, \theta)| < q$ , so the polarization process can begin immediately. We also show in Table IV results when  $k \neq 0$ . We again find that the results are not very sensitive to the anisotropic initial conditions, although we did not carry out an exhaustive study over the full range of the many variables. Thus, for example, as  $\tau_R^* \rightarrow \infty$  (or alternatively as  $\tau_R^{*eff} \rightarrow \tau_1^*$ ), one might expect somewhat enhanced effects.<sup>18</sup>

When the experimentally determined ratios of polarization due to geminate and random initial processes were compared to the theoretical values of Paul<sup>16</sup> excellent agreement was found. From our discussion and the results in Table IV we would predict about a 10% deviation in observed polarizations if highly anisotropic initial conditions existed for geminate radical pairs. The polarizations from F pairs, as noted, should be well predicted by earlier theories.<sup>2</sup> However, since good agreement was found between observed and calculated ratios there appears to be no discrepancy in the prediction of geminate pair polarizations by the simpler theory. This is evidence that the geminate pairs in this system must randomly orient before polarization processes commence.

## VI. Conclusions

We have, in this work, succeeded in extending the Pedersen-Freed theory for CIDN(E)P to cover the case of orientation-dependent interactions, and we have largely confirmed their qualitative predictions. The simple case, where one of the two radicals exhibits isotropic behavior and the anisotropic behavior of the other obeys a simple functional form, was analyzed in detail, although the approach may be generalized to more complex situations.

We have found that the primary effect on CIDNP of an anisotropic reactivity is the reduction in  $\Lambda$ , the reaction probability for the full collision, that can be rather accurately approximated by the use of an "effective" spherically symmetric specific rate constant, which, however, is a function of  $Rd^2/D$ , because of the role played by rotational reencounters. This immediately implies that one can use a spherically symmetric theory for CIDNP (but with a "renormalized"  $\Lambda$ ) to interpret experiments.

In the case of CIDEP in the absence of reactivities, we generally find that the orientation dependence of  $J(r, \theta)$  has virtually no effect on the values of the polarizations that are asymptotic with large  $J(r, \theta)$  provided the correct "effective" spherically symmetric exchange interaction is used. However, there are some changes in the magnitude of  $P_a^\infty$  (varying by about  $\pm 50\%$ ) and a greater breadth of  $P_a^\infty$  vs.  $J(r, \theta)$  about this maximum ( $P_a^\infty$  max). [Somewhat larger effects might be anticipated from more sharply orientational varying functional forms, but they were not studied.] In the presence of orientation-dependent reactivities,  $K(r, \theta)$ , such that  $K(r, \theta)$  shows substantially greater orientation dependence than  $J(r, \theta)$  (and  $\Lambda < 1$ ), then deviations by as much as factors of 2 or 3 from the asymptotic  $P_a^\infty$  are found, and even greater effects might be expected for more sharply varying functional forms for  $K(r, \theta)$ . It is this situation which might have some relevance for the recent CIDEP observations by Paul.

In general, we find that anisotropic initial conditions have only a small effect on the polarizations, largely because rotational relaxation is an effective mechanism for quickly relaxing these initial conditions for typical values of  $Rd^2/D$ . For more realistic models that include anisotropic interaction potentials affecting the reorientation,

we would again expect that the initial conditions would relax rapidly to the anisotropic equilibrium relative orientational distribution, so that initial conditions should not be too important, but there should otherwise be important effects on  $\Lambda$  (hence  $\mathcal{F}$ ) as well as  $P_a^\infty$  (for  $k \neq 0$ ) from the anisotropic interaction potentials.

In general, then, we expect that the general trends we have observed in our simple cases will carry over to more complex models, although it would be interesting to study models with more asymmetric reactivity and with asymmetric shapes.

Finally we note that our approach can be effectively employed in a variety of problems in chemical physics and biophysics.<sup>19</sup>

*Acknowledgment.* The authors express their thanks to Henning Paul for sending the preprint of his study. This work was supported by NSF Grant 77-26996.

## Appendix A

The general SLE appropriate to our problem is (cf. eq 2.1)

$$\rho(\vec{r}_i, t) = -i\mathcal{H}_0^* \rho(\vec{r}_i, t) - i\mathcal{H}_j^*(\vec{r}_i) \rho(\vec{r}_i, t) + D\Gamma_{\vec{r}} \rho(\vec{r}_i, t) + \sum_{j=1,2} R_j \Gamma_{r_j} \rho(\vec{r}_i, t) + k(\vec{r}_i) \rho(\vec{r}_i, t) \quad (\text{A1})$$

where  $\vec{r}$  is short-hand notation for  $\vec{r}$ , the internuclear vector, as well as the orientations of molecules 1 and 2 relative to the lab frame specified by Euler angles  $\Omega_1$  and  $\Omega_2$ , respectively, while  $D\Gamma_{\vec{r}}$  and  $R_j \Gamma_{r_j}$  are the translational and rotational diffusion operators, respectively. We now assume axial symmetry of each molecule with respect to its reactivity (for simplicity) so that  $\Omega_1 \rightarrow \beta_1, \gamma_1$  and  $\Omega_2 \rightarrow \beta_2, \gamma_2$ , i.e., the polar and azimuthal angles, respectively. Thus we can regard the spherical harmonics  $Y_{L_1 m_1}(\beta_1, \gamma_1)$  and  $Y_{L_2 m_2}(\beta_2, \gamma_2)$  as bases of representation of  $\rho(\vec{r}, t)$ . [More generally we would need the generalized spherical harmonics  $\mathcal{D}_{k_1 m_1}^{L_1}(\Omega_1)$  and  $\mathcal{D}_{k_2 m_2}^{L_2}(\Omega_2)$ .] It is more convenient to use a coupled representation such as<sup>10</sup>

$$|L_1, L_2, J, M\rangle = \sum_{m_1, m_2} Y_{L_1 m_1}(\beta_1, \gamma_1) Y_{L_2 m_2}(\beta_2, \gamma_2) (L_1 m_1 L_2 m_2 | L_1 L_2 J M) \quad (\text{A2})$$

where  $(L_1 m_1 L_2 m_2 | L_1 L_2 J M)$  are the vector coupling coefficients. Actually eq A2 is not precisely of the form needed, since, in general,  $J(\vec{r}_i)$  and  $k(\vec{r}_i)$  will have angular dependences such that they may be expanded in terms of the Legendre polynomials  $P_L(\cos \theta_i)$ . We consider as an example the case where  $J(\vec{r}_i)$  and  $k(\vec{r}_i)$  depend only on the orientations of each molecule with respect to the internuclear axis. Then we may expand either function (written as  $f(\vec{r}_i, \Omega_1, \Omega_2)$ ) in terms of the Legendre polynomials,  $P_L(\cos \theta_i)$ :

$$f(\vec{r}, \Omega_1, \Omega_2) = \sum_{L_1, L_2} C_{L_1, L_2}(r) P_{L_1}(\cos \theta_1) P_{L_2}(\cos \theta_2) \quad (\text{A3})$$

where  $\theta_1$  and  $\theta_2$  represent the angles between the symmetry axis of molecule 1 and 2, respectively, and  $\vec{r}$  (which may be represented by  $r = |\vec{r}|$ ,  $\beta$ , and  $\gamma$ ). It follows from the spherical Harmonic addition theorem that

$$f(\vec{r}, \Omega_1, \Omega_2) = (4\pi)^2 \sum_{\substack{L_1, L_2 \\ m_1, m_2}} \left\{ \frac{C_{L_1, L_2}(r)}{(2L_1 + 1)(2L_2 + 1)} \times Y_{L_1 m_1}^*(\beta_1, \gamma_1) Y_{L_2 m_2}^*(\beta_2, \gamma_2) Y_{L_1 m_1}(\beta_1, \gamma_1) Y_{L_2 m_2}(\beta_2, \gamma_2) \right\} = (4\pi)^{3/2} \sum_{L_1, L_2, L'} \left( \frac{2L' + 1}{(2L_1 + 1)(2L_2 + 1)} \right)^{1/2} \begin{pmatrix} L_1 & L_2 & L' \\ 0 & 0 & 0 \end{pmatrix} \times C_{L_1, L_2}(r) Q(L_1, L_2, L') \quad (\text{A4a})$$

where

$$Q(L_1, L_2, L') \equiv \sum_{m_1, m_2, m'} \begin{pmatrix} L_1 & L_2 & L' \\ m_1 & m_2 & m' \end{pmatrix} \times Y_{L_1, m_1}^*(\beta_1, \gamma_1) Y_{L_2, m_2}^*(\beta_2, \gamma_2) Y_{L', m'}^*(\beta, \gamma) \quad (\text{A4b})$$

$$\cos \theta_i = \cos \beta_i \cos \beta + \sin \beta_i \sin \beta \cos (\gamma_i - \gamma) \quad (\text{A4c})$$

We are using the 3j symbol:

$$\begin{pmatrix} L_1 & L_2 & J \\ m_1 & m_2 & m \end{pmatrix} \equiv (-1)^{L_1 - L_2 - m} (2L + 1)^{1/2} \times (L_1, m_1, L_2, m_2 | L, L_2, J, -m) \quad (\text{A5})$$

It follows from the general properties of 3j symbols (Edmonds<sup>10</sup> eq 6.2.1) or alternatively from the scalar properties of  $J$  and  $K$  that  $Q(L_1, L_2, L')$  is a scalar quantity. Thus, the effects of  $J(\vec{r}_i)$  and  $K(\vec{r}_i)$  will be independent of the azimuthal quantum numbers  $(m_1, m_2, m', M)$ . It follows from eq A4 that the proper coupled representation involves the coupling of the three bases  $Y_{L_1, m_1}(\beta_1, \gamma_1)$ ,  $Y_{L_2, m_2}(\beta_2, \gamma_2)$ , and  $Y_{L, m}(\beta, \gamma)$  which can be achieved by standard means.<sup>10</sup> The advantage of the coupled representation is that it enables one to take maximum advantage of the spherical symmetry of the problem (e.g., the invariance to  $m_1, m_2, m', M$ ). Since the coupling of three angular momenta somewhat complicates the analysis, we instead treat in detail the simpler problem, which is sufficient for the present work, viz. the case where molecule 2 exhibits spherically symmetric behavior, so that eq A3 becomes

$$f(\vec{r}_1, \Omega_1, \Omega_2) = \sum_{L_1} C_{L_1}(r) P_{L_1}(\cos \theta_1) = (4\pi) \sum_{L_1, L} \frac{C_{L_1}(r)}{(2L_1 + 1)} Y_{L_1, m_1}^*(\beta_1, \gamma_1) Y_{L_1, m_1}(\beta, \gamma) \quad (\text{A6})$$

We thus use as our coupled representation

$$|L, L_1, J, M\rangle = \sum_{m, m_1} Y_{L, m}(\beta, \gamma) Y_{L_1, m_1}(\beta_1, \gamma_1) (L, m, L_1, m_1 | L, L_1, J, M) \quad (\text{A7})$$

in order to expand  $\rho(\vec{r}_i, t)$  as

$$\rho(\vec{r}_i, t) = \sum_{L, L_1, J, M} \rho(L, L_1, J, M, r, t) |L, L_1, J, M\rangle \quad (\text{A8})$$

where  $\rho(L, L_1, J, M, r, t)$  is still a spin operator and is  $r$  dependent. Now, because of spatial isotropy, orientations  $\beta$  and  $\gamma$  as well as  $\beta_1$  and  $\gamma_1$  are equally probable. (We are neglecting any anisotropic coupling between the rotation of molecule 1 and the relative translational motion.) Thus the observables will depend only upon

$$\frac{1}{(4\pi)^2} \int \int d\beta d\gamma \int \int d\beta_1 d\gamma_1 \rho(\vec{r}_i, t) = \langle 0, 0, 0, 0 | \rho(\vec{r}_i, t) | 0, 0, 0, 0 \rangle = \rho(0, 0, 0, 0, r, t) \equiv \rho_0(r, t) \quad (\text{A9})$$

We now consider the various matrix elements of eq A1 in this coupled representation starting with eq A6. In particular, we have (cf. ref 10, p 114)

$$\langle L', L_1', J', M' | P_l(\cos \theta_1) | L, L_1, J, M \rangle = (-1)^{L+L_1'+J} \delta_{J, J'} \delta_{M, M'} \begin{Bmatrix} J & L_1 & L' \\ l & L & L_1 \end{Bmatrix} \times [(2L+1)(2L'+1)(2L_1+1)(2L_1'+1)]^{1/2} \times \begin{pmatrix} L & l & L' \\ 0 & 0 & 0 \end{pmatrix} \begin{pmatrix} L_1 & l & L_1' \\ 0 & 0 & 0 \end{pmatrix} \quad (\text{A10})$$

where we have introduced the 6j symbol by the curly brackets. Thus  $J$  and  $M$  are invariant quantum numbers for terms in the expansion eq A6. We now consider  $R_1 \Gamma_{\Omega_1}$  (and ignore any potential terms for simplicity) whose eigenfunctions are the spherical harmonics. That is, in the

uncoupled representation

$$R_1 \Gamma_{\Omega_1} Y_{L_1, m_1}(\theta, \varphi) = R_1 L(L+1) Y_{L, m}(\theta_1, \varphi_1) \quad (\text{A11})$$

[This result can easily be generalized to a molecule exhibiting axially symmetric rotational diffusion relative to its principal symmetry axis. Since it is only rotation of this axis which is of interest in the present problem, we may let  $R_1 \rightarrow R_{\perp}$ , the perpendicular component of the diffusion tensor.] Because of the independence of the eigenvalues on  $m_1$  in eq A11, it immediately follows that in the coupled representation

$$\langle L', L_1', J', M' | R_1 \Gamma_{\Omega_1} | L, L_1, J, M \rangle = R_1 L_1 (L_1 + 1) \delta_{L, L'} \delta_{L_1, L_1'} \delta_{J, J'} \delta_{M, M'} \quad (\text{A12})$$

Similarly we may consider

$$\Gamma_{\vec{r}} = \Gamma_r + (1/r^2) \Gamma_{\Omega} \quad (\text{A13a})$$

where  $\Omega \rightarrow \beta, \gamma$  and

$$\left\langle L', L_1', J', M' \left| \frac{D}{r^2} \Gamma_{\Omega} \right| L, L_1, J, M \right\rangle = \frac{D}{r^2} L(L+1) \delta_{L, L'} \delta_{L_1, L_1'} \delta_{J, J'} \delta_{M, M'} \quad (\text{A13b})$$

It follows from eq A10–A13 that the terms in eq A1 will only couple in coefficients of the  $|L, L_1, 0, 0\rangle$  kets into the equilibrium ket  $|0, 0, 0, 0\rangle$ , where the precise nature of these kets is determined by eq A10. Thus, if we set  $J = 0$  in the 6j symbol of eq A10 it immediately follows from its "triangle rules" that  $L = L_1$  and  $L_1' = L'$  for this symbol to be nonzero, and then

$$\begin{Bmatrix} 0 & L' & L' \\ l & L & L \end{Bmatrix} = [(2L+1)(2L'+1)]^{-1/2} \quad (\text{A14})$$

where from 3j symbols in eq A10  $L' = L + l, L + l - 2, \dots, |L - l + 2|, |L - l|$ . Thus, from the further symmetry contained in the 6j symbols we see that only kets  $|L, L, 0, 0\rangle$  couple into the problem, i.e., only one quantum number:  $L$  is relevant (out of the initial four). In particular for  $l = 1$ , we have  $L' = L \pm 1$  and

$$\langle L', L_1', J', M' | P_1(\cos \theta_1) | L, L_1, J, M \rangle = -\delta_{J, J'} \delta_{M, M'} \delta_{L, L'} \delta_{L_1, L_1'} \left[ \frac{L}{[(2L-1)(2L+1)]^{1/2}} \delta_{L, L'+1} + \frac{L+1}{[(2L+1)(2L+3)]^{1/2}} \delta_{L, L'-1} \right] \quad (\text{A15})$$

while the combination of eq A12 and A13b becomes

$$\left\langle L, L, 0, 0 \left| R_1 \Gamma_{\Omega_1} + \frac{D}{r^2} \Gamma_{\Omega} \right| L, L, 0, 0 \right\rangle = \left( R_1 + \frac{D}{r^2} \right) L(L+1) \quad (\text{A16})$$

thus proving the additivity of these terms, which was assumed in the simplified analysis of section II. (Compare also eq A15 with eq 2.19a obtained by the simplified analysis.)

This approach, when generalized to the case of eq A3, should yield a dependence on two quantum numbers (essentially representing the angles  $\theta_1$  and  $\theta_2$ ), while a more general expansion than eq A.3, allowing for the relative phase of  $\theta_1$  vs.  $\theta_2$  about  $\vec{r}$ , would introduce a third quantum number. Also our above treatment could be generalized to the inclusion of orientation-dependent potential terms  $U(\vec{r}, \theta_1, \theta_2)$  in the operators  $D \Gamma_{\vec{r}}$  and  $R_i \Gamma_{\Omega_i}$  (cf. eq 2.1). [A discussion somewhat related to that of this Appendix appears in ref 4a.]

